Applied Physics Letters

Thickness-dependent electron momentum relaxation times in iron films

Cite as: Appl. Phys. Lett. **116**, 102406 (2020); https://doi.org/10.1063/1.5142479
Submitted: 13 December 2019 • Accepted: 24 February 2020 • Published Online: 10 March 2020

K. L. Krewer, W. Zhang, J. Arabski, et al.

COLLECTIONS

This paper was selected as an Editor's Pick

View Online

Export Citation

CrossMark

ARTICLES YOU MAY BE INTERESTED IN

Thermally modulated hydrogenation in Fe_xPd_{1-x} alloy films: Temperature-driven peculiar variation of magnetism
Applied Physics Letters **116**, 102407 (2020); https://doi.org/10.1063/1.5142625

Electron mean free path in elemental metals
Journal of Applied Physics **119**, 085101 (2016); https://doi.org/10.1063/1.4942216

A unified model for vertical doped and polarized superjunction GaN devices
Applied Physics Letters **116**, 102103 (2020); https://doi.org/10.1063/1.5142855

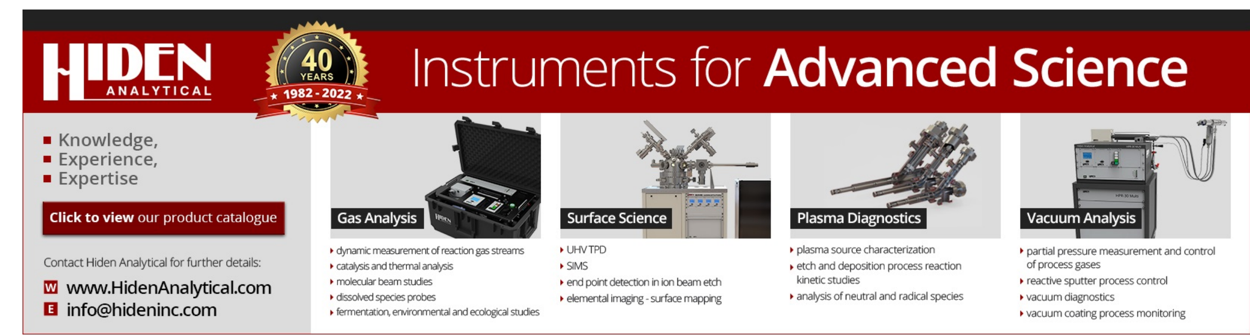

© 2020 Author(s).

Applied Physics Letters ARTICLE scitation.org/journal/apl

Thickness-dependent electron momentum relaxation times in iron films

Cite as: Appl. Phys. Lett. **116**, 102406 (2020); doi: 10.1063/1.5142479
Submitted: 13 December 2019 · Accepted: 24 February 2020 ·
Published Online: 10 March 2020

View Online

Export Citation

CrossMark

K. L. Krewer,[1,2,a)] W. Zhang,[1,3] J. Arabski,[4] G. Schmerber,[4] E. Beaurepaire,[4] M. Bonn,[1] and D. Turchinovich[1,3]

AFFILIATIONS

[1]Max Planck Institute for Polymer Research, 55128 Mainz, Germany
[2]Graduate School of Excellence Material Science in Mainz, 55128 Mainz, Germany
[3]Fakultät für Physik, Universität Bielefeld, 33615 Bielefeld, Germany
[4]Université de Strasbourg, CNRS, Institut de Physique et Chimie des Matériaux de Strasbourg, UMR 7504, 23 Rue du Loess, F-67000 Strasbourg, France

[a)]Author to whom correspondence should be addressed: krewer@mpip-mainz.mpg.de

ABSTRACT

Terahertz time-domain conductivity measurements in 2–100 nm thick iron films resolve the femtosecond time delay between the applied electric fields and the resulting currents. This current response time decreases from 29 fs for the thickest films to 7 fs for the thinnest films. The macroscopic response time is not strictly proportional to the conductivity. This excludes the existence of a single relaxation time universal for all conduction electrons. We must assume a distribution of microscopic momentum relaxation times. The macroscopic response time depends on the average and variation of this distribution; the observed deviation between the response time and conductivity scaling corresponds to the scaling of the variation. The variation of microscopic relaxation times depends on the film thickness because electrons with different relaxation times are affected differently by the confinement since they have different mean free paths.

© 2020 Author(s). All article content, except where otherwise noted, is licensed under a Creative Commons Attribution (CC BY) license (http://creativecommons.org/licenses/by/4.0/). https://doi.org/10.1063/1.5142479

Conductivity in metals is typically described using a highly simplified model: a gas of identical electrons characterized by a single, universal relaxation time.[1–4] This contrasts with the complexity of the underlying process where all electronic states on the Fermi surface contribute to conduction,[3,5] and relaxation times often vary strongly across the Fermi surface.[6–10] The time delay of a few femtoseconds between an applied field and the resulting current—the current response time τ_C—reflects the macroscopic momentum relaxation of an ensemble of charges. Resolving this delay can, therefore, provide insights into the relaxation processes and connect microscopic scattering to macroscopic conduction.

This is particularly relevant for thin metal films[1,2,4,11–13] for which different electrons can be affected differently by confinement. Here, we determine τ_C as a function of thickness for thin metal films and demonstrate that different types of electrons with different relaxation times are present in the films.

We performed substrate referenced transmission terahertz time-domain transmission spectroscopy[14,15] at room temperature (293 K) on iron films with thicknesses ranging from 2.2 to 100 nm. The films were deposited on double-polished MgO (100) substrates and capped with ca. 12 nm of MgO. The films were grown by molecular beam epitaxy at room temperature, with subsequent annealing. The thicknesses *a* were controlled *in situ* by quartz balance sensing and confirmed *ex situ* by small-angle x-ray diffraction (XRD) for selected samples (see supplementary material Fig. S1). Roughnesses extracted from the XRD are on average 0.9 ± 0.1 nm, without a significant dependence on the thickness. Reflection high-energy electron diffraction images indicate that this preparation method achieves single-crystalline films with a bcc lattice structure (see Figs. S2 and S3 in the supplementary material).

Terahertz radiation was generated and detected in 1 mm ZnTe crystals using 800 nm 40 fs pulses from an amplified Ti:sapphire laser emitting 1000 pulses per second.[14] We alternated recording the terahertz transmission through the samples with the transmission through a bare reference substrate. We performed three rounds of measurements, each with a different combination of samples, alternatingly acquiring traces for the sample and reference 10–30 times. We corrected the terahertz transmission relative to the reference substrate for substrate thickness differences.[16] We then numerically solved the transfer matrices[17] for the corrected transmission data, using the thin conductive film approximation[15,18] to generate starting values. This approach allows reliably determining the phase φ of the conductivity $\tilde{\sigma}$, even for films for which the phase acquired by the terahertz pulse

© Author(s) 2020

during a direct transit is non-negligible (see the supplementary material).

The current response time τ_C can be obtained from the measured phase φ of the conductivity $\tilde{\sigma}$ at a specific frequency f, through

$$\tau_C(f) = \tan(\varphi(\tilde{\sigma}(f)))/(2\pi f). \quad (1)$$

If a universal relaxation time τ_u existed, the current response time τ_C would be constant and equal to the universal relaxation time τ_u of the Drude model. Previous measurements of the current response time in metals were limited to ca. 10 fs accuracy, due to uncertainties in the thickness of the reference substrate.[19,20] Our thickness correction technique allows determining the current response time with an error of ca. 1 fs[16] for most cases, allowing to compare response times between different samples. Figure 1 shows three exemplary phase-resolved conductivity spectra for a very thin (2.2 nm), an intermediate (10.3 nm), and a thick film (100 nm). The phase-resolved conductivity is plotted in terms of amplitude σ and current response time τ_C. The spectra are essentially flat, with the exception of the conductivity amplitude σ of the 100 nm film, which slightly decreases with increasing frequency. Deviations from flat spectra are larger than the statistical errors and correlate between different samples; for example, an increase in response time τ_C for high frequencies occurs for both the 2.2 and 10 nm films shown in Fig. 1. These residuals only correlate between different samples measured in the same round; the residuals do not correlate with the same samples measured in a different round several months later with a different reference substrate (see supplementary Fig. S4). Therefore, we consider these residuals as artifacts.

The amplitude spectra $\sigma(f)$ are flat due to the very low relaxation times τ. The flat response time spectra $\tau_C(f)$ appear to be consistent with the hypothesis of a universal relaxation time τ_u, as the hypothesis

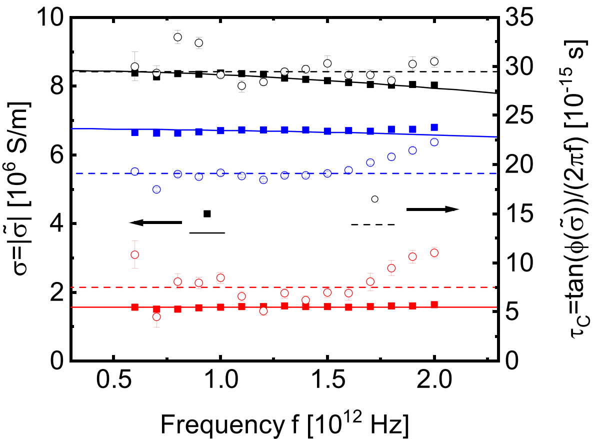

FIG. 1. The complex conductivities $\tilde{\sigma}$ extracted from time-domain spectroscopy, represented as amplitude σ (full squares, left axis) and current response time τ_C (empty circles, right axis), which are the tangent of the phase over angular frequency. Conductivity spectra are displayed for a thick (100 nm, black), intermediate (10.3 nm, blue), and very thin (2 nm, red) sample. The error bars indicate the standard error of the mean, inferred from repeated measurements. Wherever invisible, the error bars are smaller than the markers. The lines denote effective Drude responses derived from spectral averages $\overline{\tau}_C$ (dashed lines, right axis) and $\overline{\sigma}_{DC}$ (full lines, left axis) of $\tau_C(f)$ and $\sigma(f)\cdot\sqrt{\left(1+(2\pi f\overline{\tau}_C)^2\right)}$.

predicts the response time to be constant and equal to τ_u, as a universal relaxation time results in a Drude type dispersion,

$$\tilde{\sigma} = \sigma_{DC}/(1 - i2\pi f\tau_u). \quad (2)$$

The universal relaxation time assumption also predicts that the DC conductivity σ_{DC} is proportional to τ_u. We find that the conductivity amplitudes σ are lower for the thinner films, with the difference between 10 and 2.2 nm being much larger than that between 100 and 10 nm. The current response time τ_C behaves quite differently. It is also lower for thinner films, but the relative difference in response times between 100 and 10 nm is almost twice that of the conductivity amplitudes, contrary to the assumption of direct proportionality. The 2.2 nm thin film shows higher current response times than direct proportionality would predict from the conductivity amplitudes.

To compare the scaling of conductivity amplitude and response time, we extract the spectral average $\overline{\tau}_C$ of the current response times for each film. We then compute the DC-limit of the conductivity of a Drude type dispersion from each frequency step by multiplying the conductivity amplitudes σ at each frequency f with $\sqrt{\left(1+(2\pi f\,\overline{\tau}_C)^2\right)}$. The resulting spectra for the DC parameter are then also averaged. The residual artifacts are the main source of error on both the response time $\overline{\tau}_C$ and DC-conductivity $\overline{\sigma}_{DC}$ parameters extracted from each spectrum. The residuals are taken into account by multiplying the variance of the weighted averages by the reduced sum of weighted residuals. Furthermore, we use the instances where we have measurements of the same sample in different rounds to estimate the precision. These measurements deviate between 0.1 and 2.7 fs from another, i.e., slightly more than what we estimate from the residuals. We use the larger estimate where we have measurements from different rounds, and we add the average unexplained variance of $(0.8\text{ fs})^2$ to the variance from the residuals where we do not have measurements from different rounds. Furthermore, we add the variances caused by a possible 1% error in the substrate refractive index, by the uncertainty of the substrate thickness correction and the uncertainty of the film thickness a.

The thickness scaling of the extracted response time and DC-conductivity is shown in Fig. 2. From thick toward thin films, the DC

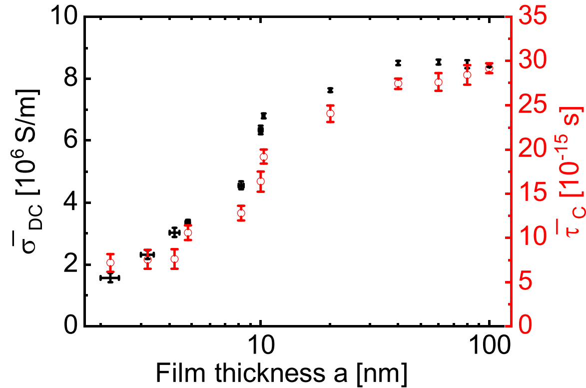

FIG. 2. DC-conductivities $\overline{\sigma}_{DC}$ (left axis, black) and current response times $\overline{\tau}_C$ (right axis, red) extracted from the complex conductivity spectra of 12 iron films from 2.2 to 100 nm thickness. The conductivity decreases and the current response becomes faster for thinner metal films, as expected from increased surface scattering, but they are not directly proportional. All measurements were performed at 293 K.

© Author(s) 2020

conductivity first hardly decreases, then jumps down from 10 to 8 nm and then keeps decreasing strongly. The current response time first decreases quickly, also jumps down from 10 to 8 nm, and then levels out toward thinner films. So while both parameters decrease with decreasing thickness a, the detailed scaling is different.

None of the existing models for the thickness scaling of conductivity predict the response time.[1,2,4,11–13] Further, the jump between 8 and 10 nm does not fit with any model. We hence do not focus on trying to find a detailed microscopic model for the exact thickness scaling of these iron films. We rather focus on the peculiarity of seeing constant current response time spectra, but no proportionality between conductivity and current response time. The spectrally constant response time is predicted by the universal relaxation time hypothesis; the deviations from proportionality contradict this hypothesis. To investigate the deviation from proportionality, we plot the quotient $Q = \bar{\tau}_C/\bar{\sigma}_{DC}$ of the response time and the DC-conductivity in Fig. 3. We see that those values are not constant, but rather start out high, decrease down to 10 nm, and increase again. We analyze how significant these deviations from proportionality are. We assume that our data obey a normal distribution. Our error bars are our best estimates for the 68% confidence interval. The best fit for a constant quotient lies several interval widths above the 68% confidence intervals for the intermediate films around 10 nm, and several times below those for 100 nm. The probability of obtaining data fitting worse than the hypothesis of a universal relaxation time is 10^{-9}, equivalent to six standard deviations for a normal distribution. The deviations are significant.

How can we explain now that the spectra of the response time are flat but the response time is not the universal relaxation time? Similar behavior has been observed by Kamal *et al.*[21] in a metal oxide film. The entire spectrum of the metal oxide can only be described by a distribution of scattering rates τ^{-1}; but for the low frequency limit, a single effective current response time suffices.[21] Similarly, we can also understand our observation by considering a distribution of

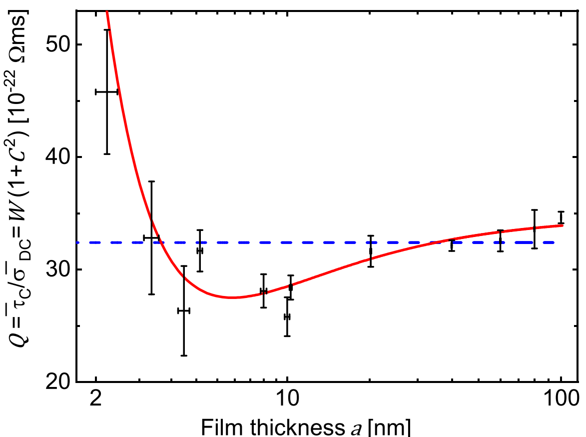

FIG. 3. Quotient Q of the current response time τ_C by the DC-conductivity σ_{DC} as a function of the film thickness. The blue dashed line is a constant fitted to the data, as predicted by the hypothesis of a universal relaxation time. The data lie outside the 99.9 99 999% (6 Gaussian standard deviations) confidence interval for the universal relaxation time hypothesis. The red curve is a second-order polynomial fit in $1/a$, consistent with two competing processes altering the variation C of the relaxation times. Data are within the 68% (1 std) confidence interval of the red curve.

microscopic relaxation times τ. We start by using the full description of the phase-resolved conductivity spectrum within the relaxation time approximation in the semi-classical Bloch–Boltzmann formalism. For a cubic crystal, this yields[3,6,22]

$$\tilde{\sigma}(f) = \frac{1}{3}\frac{e^2}{8\pi^3}\sum_{b,s}\int_0^\infty \iint_{S(\mathcal{E})} -\frac{\partial g}{\partial \mathcal{E}} v_g(\vec{S},\mathcal{E},b,s)\frac{\tau(\vec{S},\mathcal{E},b,s)}{1-i2\pi f\tau(\vec{S},\mathcal{E},b,s)} dS d\mathcal{E}. \tag{3}$$

Here, we sum over all bands b and both spin projections s and integrate over all iso-energy surfaces $S(\mathcal{E})$ in reciprocal space. The conductivity contribution for each point $\vec{S}$ on such an iso-energy surface is given by the group velocity v_g and the relaxation time τ, which both may vary between each point $\vec{S}$, energy $\mathcal{E}$, band b, and spin s.[6] The contribution is weighted by the energy derivative of the electron distribution function g; when the electron population conducts in a steady-state, this is the Fermi-distribution. The derivative of the Fermi distribution means that only electronic states close to the Fermi surface contribute. g will deviate from the Fermi distribution when the energy of the photons hf is larger than the typical thermal excitation k_BT. For room temperature (293 K), this implies frequencies f larger than 6 THz. Since we stay below 6 THz, the observables we measure only depend on the same microscopic properties which govern steady-state transport at room temperature.

The key point is that already in the semi-classical theory, the relaxation time is not necessarily universal, but varies between the electronic states contributing to conduction. Since we want to assess the phase and frequency dependence of the conductivity, we convert the integral of Eq. (3) into an integration over the relaxation times,

$$\tilde{\sigma}(f) = W^{-1}\int_0^\infty \frac{w(\tau)\tau}{1-i2\pi f\tau} d\tau. \tag{4}$$

Basically, all parameters $\vec{S}$, $\mathcal{E}$, b, and s have been expressed as functions of τ, allowing us to express the integrand as a single function $w(\tau)$. The prefactor W^{-1} is chosen such that $w(\tau)$ is normalized. This allows interpreting $w(\tau)$ as a probability distribution density. The distribution of microscopic relaxation times $w(\tau)$ gives the probability that a microscopic excitation of unit conductivity per relaxation time will relax in a time τ. W only depends on the electronic structure of the material and not on the relaxation times τ. In the case of a universal relaxation time τ_u, the distribution $w(\tau)$ reduces to a delta distribution $\delta(\tau-\tau_u)$. Inserting this in Eq. (4) and looking at the DC-limit, we identify W as the quantity $\rho_0\tau_u$ calculated by Gall[3] by integrating computed group velocities over the Fermi surface. Within Drude's assumption of a universal relaxation time and photon energy independence of $\frac{\partial g}{\partial \mathcal{E}}$, W is connected to Drude's plasma frequency ω_P via $W^{-1} = \varepsilon_0 {\omega_P}^2$.

We measure the low-frequency limit of $\tilde{\sigma}(f)$. Therefore, we Taylor-expand Eq. (4) for frequencies f lower than $1/(2\pi\tau)$,

$$\tilde{\sigma}(f) = \frac{1}{W}\sum_{l=0}^{\infty}(i2\pi f)^l\langle\tau^{l+1}\rangle, \tag{5}$$

$$= \frac{\sigma_{DC}}{1-i2\pi f\tau_C} + O\left((2\pi f\tau)^2\right). \tag{6}$$

Here, $\langle\rangle$ denotes the average over the distribution of relaxation times $w(\tau)$. Equation (5) tells us that the conductivity is directly

© Author(s) 2020

connected to the moments $\langle \tau^l \rangle$ of the relaxation time distribution $w(\tau)$. Theoretically, all moments could be inferred from the spectrum, and thereby the entire distribution. In practice, we can infer information about the first two moments: Equation (6) holds for

$$\sigma_{DC} = \frac{\langle \tau \rangle}{W} \quad \text{and} \quad \tau_C = \frac{\langle \tau^2 \rangle}{\langle \tau \rangle} = \langle \tau \rangle (1 + C^2). \tag{7}$$

The first moment, the mean relaxation time $\langle \tau \rangle$, gives us the average magnitude. The second centralized moment is the variance V. The standard deviation $\sqrt{V}$ measures the absolute width of the distribution. To decide how much impact the shape of the distribution has, we need to compare the standard deviation to the mean. This ratio $\sqrt{V}/\langle \tau \rangle$ is the coefficient of variation C. We hence can interpret the deviations of $Q = \bar{\tau}_C / \bar{\sigma}_{DC} = W(1 + C^2)$ from a constant value in Fig. 3 in terms of a change in variation C of the microscopic relaxation times.

Now, we will show that the deviations of Q from a constant value are not random, but depend systematically on film thickness a. To this end, we show that a simple polynomial function of the thickness a describes the data reasonably well. This polynomial is $Q(a) = Q_\infty - b_1/a + b_2/a^2$, displayed as the red curve in Fig. 3. The probability p of obtaining data fitting worse than this polynomial is 0.21. The expectation value of this probability is 0.5. The p value is within 0.34 (one Gaussian standard deviation) of its expected value. This indicates a good fit. The fit parameters are $Q_\infty = 34.8 \times 10^{-22}\,\Omega\,\text{ms}$, $b_1 = 9.2 \times 10^{-15}\,\Omega\,\text{s}$, and $b_2 = 2.9 \times 10^{-6}\,\Omega\,\text{s/m}$. This description with a simple polynomial function shows that the thickness scaling of Q is systematic.

Next, we describe two effects by which surface scattering may alter the variation C of microscopic relaxation times and thereby qualitatively explain the thickness scaling of Q. First, the anticorrelation of bulk and surface scattering may decrease C. Surface scattering predominantly affects electrons with a long expected free path, since those electrons are most likely to reach the surface instead of scattering in bulk. This anticorrelation starts cutting off the long relaxation time "tail" of the distribution of microscopic relaxation times, which decreases the variation. The thinner the film, the larger the role of surface scattering and the larger the reduction of the variation from bulk scattering by the anticorrelated surface scattering. We can interpret the b_1-term in the empirical polynomial as representing this narrowing of the relaxation time distribution by anticorrelated scattering mechanisms.

Second, the surface scattering will add positional (z) and directional (v_z) variation between microscopic relaxation times $\tau(\vec{S}, \mathcal{E}, b, s, z, v_z)$. An electron may scatter very soon from the surface when it is close to the surface and travels toward the surface. An electron that is far away from the surface or traveling parallel to the surface will hardly scatter from it. So the relaxation times due to surface scattering will vary strongly, and the directional variation will increase for increasingly thinner films. This variation will add to the intrinsic variation, increasing the total variation C. We can motivate the b_2 term by this effect. We should mention that contrary to the decrease in Q from 100 to 8 nm, the strong rise of Q for the thinnest films is much less significant due to large uncertainties. Further, competing explanations for this increase exist. First, at thicknesses of a few nm, the roughness of almost 1 nm will cause systematic errors, as described by Namba.[23] Second, recent x-ray absorption measurements on a 1.5 nm film[24] suggest some changes to the electronic structure for such a thin film compared to the bulk. This means for the thinnest films, the value of W may change.

We now check whether our explanation of two mechanisms changing the variation of relaxation times is consistent with the observed conductivity scaling: When surface scattering dominates, the increase in directional variation will increase Q with decreasing thickness. When bulk scattering dominates, the anticorrelation effect will decrease the variation with decreasing thickness. Therefore, a minimum in variation C and quotient Q should occur when bulk and surface scattering contributions are about equal, which implies a conductivity of ca. half the bulk value. In our measurement, the conductivity drops to half the value of the thickest film between 5 and 8 nm film thickness a, which coincides with the minimum the empirical $Q(a)$ scaling. So we have found a qualitative explanation for how surface scattering can cause the scaling of the variation C and therefore the observed scaling of Q, and this explanation is consistent with the scaling of the conductivity.

Last but not least, we check the consistency of the variation scaling explanation by comparing Q_∞ to values of W calculated from the electronic band structure. The anticorrelation between bulk and surface scattering can only take effect when a large variation C_∞ exists in bulk, which implies that Q_∞ must be larger than W. Cazzaniga *et al.*[25] use the density functional theory with local spin density approximation to calculate a dc-conductivity σ_{DC} of 155×10^6 S/m for an assumed universal relaxation time τ_u of 143 fs, from which we can calculate a value for $W = \tau_u/\sigma_{DC}$ of $9.2 \times 10^{-22}\,\Omega\,\text{ms}$. For nickel, a cubic ferromagnet like iron, Gall[3] reports a similar calculated value of $10.0 \times 10^{-22}\,\Omega\,\text{ms}$. Cazzaniga's value for W is 3.8 times smaller than the $34.8 \times 10^{-22}\,\Omega\,\text{ms}$ we observe for $Q_\infty = W(1 + C_\infty{}^2)$. This translates to a variation C_∞ of 1.7 in bulk; that means the standard deviation of the relaxation time distribution is 1.7 times larger than the mean. This variation would certainly be large enough for narrowing of the relaxation time distribution by anticorrelated surface scattering to occur.

We illustrate the impact of the variation of microscopic relaxation times on the current response time by using Cazzaniga's value for W to estimate the mean relaxation time $\langle \tau \rangle$ from the conductivity of the 100 nm film. We estimate 8 fs, while the observed current response time $\bar{\tau}_C$ is 29 fs.

In summary, we have resolved the phase of the THz conductivity of iron films with enough precision to demonstrate decreasing current response times $\bar{\tau}_C$ with the decreasing thickness. We could further resolve significant deviations between the scaling of the DC-conductivity and the response time. This can happen when no universal relaxation time τ_u exists. At this point, we need to distinguish between the observable macroscopic response time τ_C, the various microscopic relaxation times τ, and the mean relaxation time $\langle \tau \rangle$ parameterizing DC-conduction. The conductivity spectrum can be fully described by the distribution $w(\tau)$ of microscopic relaxation times. For the low-frequency limit, the observable DC-conductivity depends on the mean $\langle \tau \rangle$, the response time on mean $\langle \tau \rangle$ and variation C of the distribution of relaxation times. We explain the thickness scaling of the quotient $Q = \tau_C/\sigma_{DC}$ by surface scattering, changing the shape of the distribution of relaxation times.

The relaxation time distribution picture allows predicting the response time τ_C for other metallic systems: Mott[7] explained the temperature-independent conduction in Constantan and Manganin

© Author(s) 2020

alloys by a process that changes the distribution, but not the average relaxation time. Therefore, the response time τ_C should increase with temperature in these alloys.

See the supplementary material for iron film characterization, terahertz data treatment, and spectral averaging/residual spectra.

We are grateful to Eduard Unger for automatizing the measurements and to Zoltan Mics and Ivan Ivanov for building the high precision setup. K.K. acknowledges the support from MAINZ-Graduate School of Excellence Material Science in Mainz. D.T. acknowledges the project "Nonequilibrium dynamics in solids probed by terahertz fields" funded by the Deutsche Forschungsgemeinschaft (DFG, German Research Foundation)-Projektnummer 278162697-SFB 1242.

REFERENCES

[1]K. Fuchs, Math. Proc. Cambridge Philos. Soc. **34**, 100 (1938).
[2]E. H. Sondheimer, Adv. Phys. **1**, 1 (1952).
[3]D. Gall, J. Appl. Phys. **119**, 085101 (2016).
[4]A. F. Mayadas and M. Shatzkes, Phys. Rev. B **1**, 1382 (1970).
[5]A. A. Abrikosov, *Fundamentals of the Theory of Metals*, 1988 ed. (North-Holland, Amsterdam, 1988).
[6]A. B. Pippard, Rep. Prog. Phys. **23**, 176 (1960).
[7]N. F. Mott, Proc. R. Soc. London, Ser. A **153**, 699 (1936).
[8]A. Fert and I. A. Campbell, Phys. Rev. Lett. **21**, 1190 (1968).
[9]D. H. Lowndes, K. Miller, and M. Springford, Phys. Rev. Lett. **25**, 1111 (1970).
[10]M. Springford, Phys. Condens. Matter **19**, 1 (1975).
[11]J. J. Thomson, Proc. Cambridge Philos. Soc. **11**, 120 (1901).
[12]N. Trivedi and N. W. Ashcroft, Phys. Rev. B **38**, 12298 (1988).
[13]R. C. Munoz and C. Arenas, Appl. Phys. Rev. **4**, 011102 (2017).
[14]R. Ulbricht, E. Hendry, J. Shan, T. F. Heinz, and M. Bonn, Rev. Mod. Phys. **83**, 543 (2011).
[15]R. D. Averitt and A. J. Taylor, J. Phys.: Condens. Matter **14**, R1357 (2002).
[16]K. L. Krewer, Z. Mics, J. Arabski, G. Schmerber, E. Beaurepaire, M. Bonn, and D. Turchinovich, Opt. Lett. **43**, 447 (2018).
[17]C. C. Katsidis and D. I. Siapkas, Appl. Opt. **41**, 3978 (2002).
[18]R. E. Glover and M. Tinkham, Phys. Rev. **104**, 844 (1956).
[19]M. Walther, D. G. Cooke, C. Sherstan, M. Hajar, M. R. Freeman, and F. A. Hegmann, Phys. Rev. B **76**, 125408 (2007).
[20]B. G. Alberding, G. P. Kushto, P. A. Lane, and E. J. Heilweil, Appl. Phys. Lett. **108**, 223104 (2016).
[21]S. Kamal, D. M. Kim, C. B. Eom, and J. S. Dodge, Phys. Rev. B **74**, 165115 (2006).
[22]N. W. Ashcroft and N. D. Mermin, *Solid State Physics* (Saunders College Publishing, Philadelphia, 1976).
[23]Y. Namba, Jpn. J. Appl. Phys., Part 1 **9**, 1326 (1970).
[24]S. Ueda, M. Mizuguchi, M. Tsujikawa, and M. Shirai, Sci. Technol. Adv. Mater. **20**, 796 (2019).
[25]M. Cazzaniga, L. Caramella, N. Manini, and G. Onida, Phys. Rev. B **82**, 035104 (2010).

© Author(s) 2020